AIMS Geosciences, 9(1): 95–122.
DOI: 10.3934/geosci.2023007
Received: 14 October 2022
Revised: 11 January 2023
Accepted: 27 January 2023
Published: 03 February 2023

http://www.aimspress.com/journal/geosciences

Research article

Combining NSP- and CPTu-based N_{kt} to evaluate undrained shear strength

Gerardo W Quirós[1,*], Patricia M Peters[2] and Kuat C Gan[3]

[1] GWQ Geotechnics, Inc., Houston, TX 77055 USA
[2] Fugro USA Marine, Inc. (retired), Houston, TX 77081 USA
[3] Fugro USA Marine, Inc., Houston, TX 77081 USA

* **Correspondence:** Email: bquiros@fugro.com; Tel: +17135983148.

Abstract: A procedure for estimating reliable ranges of N_{kt} for direct simple shear (DSS)-based and anisotropically consolidated triaxial compression (CAUC)-based undrained shear strength is presented. The procedure is based on a combination of three Normalized Soil Parameter (NSP) methods and two CPTu (piezocone penetrometer) methods and are related to the ratio of net cone resistance to hydrostatic effective vertical stress. The NSP and CPTu data used were acquired from seven sites: these sites have stress histories ranging from very underconsolidated to very highly overconsolidated. The stratigraphies of the seven sites consist of clays that are moderately plastic to highly plastic. This proposed procedure was then applied to 22 published sites with a wide range of fine-grained soil types and index properties. The procedure yielded very consistent and reasonable envelopes of N_{kt}, which in turn, provide sound DSS-based strength profiles as well as CAUC-based strength profiles. The proposed procedure also clearly demonstrates that the range for N_{kt} factors is not limited to 15 to 20 for normally consolidated to lightly overconsolidated cohesive sediments, which is frequently employed by practitioners.

Keywords: in situ testing; normalized soil parameters; soft to hard clays; soil sampling effects; stress history; undrained shear strength

1. Introduction

Factors such as the presence of gas and silt or sand inclusions in sediments, sample stress relief, vessel motion when sampling offshore, and drilling methods or constraints can significantly affect sample quality in a geotechnical investigation [1]. Lower sample quality, consequently, results in lower standard laboratory undrained shear strength (s_u) measurements [2]. However, applications of data from the piezocone penetrometer (CPTu) and Normalized Soil Parameter (NSP) laboratory tests are priceless tools that the geotechnical practitioner can employ to better assess the in situ s_u of cohesive sediments. The CPTu and NSP methods are both used to evaluate undrained shear strength; both require stress history but are based on two different laboratory strength tests. Recent researchers have related CPTu cone response to CAUC triaxial tests (Mayne and Peuchen [3]) and stress history (Agaiby and Mayne [4]). NSP methods are based solely on laboratory-based undrained shear strength and stress history. Over the past 6 years, the authors have successfully employed the procedure recommended in this paper (NSP-CPTu Method) to evaluate in situ s_u, particularly in offshore regions where there has been little infrastructure development and, therefore, a lack of geotechnical experience with the sediments encountered. The procedure described in subsequent sections incorporates two CPTu-based methods: one published by Mayne et al. [5] and another by Mayne and Peuchen [3]. Additionally, the procedure also combines three NSP laboratory methods: two proposed by Quiros et al. [6] and another proposed by Casey and Germaine [7]. The authors have found that the results from these five methods yield a narrow range of N_{kt} values that provide in situ s_u interpretations that are quite reasonable and justifiably less conservative than those often used in practice. The procedure was also applied to 22 published sites, and a table of the results is presented.

2. Approach

Despite our industry's best practices, the process of drilling and soil sampling disturbs the soil from its natural state to varying degrees. Stress relief during the sampling process can cause expansion and disturbance as gas comes out of the solution [8]. Every soil has a unique susceptibility to disturbance by sampling depending on deposition, mineralogy, and geology. In addition, sample disturbance can affect diverse laboratory tests differently. In situ data, specifically CPTu, and advanced laboratory testing programs aid in evaluating a far more realistic undrained shear strength than standard strength testing on samples alone.

The undrained shear strength, s_u, derived from CPTu data is determined according to the following relationship:

$$s_u = q_{net}/N_{kt} \tag{1}$$

where q_{net} is net cone resistance (corrected for hydrostatic and transient pore pressures, in situ stress, and cone shape) and N_{kt} is the dimensionless bearing capacity factor for the cone penetrometer. A statistical approach, together with engineering judgment, is sometimes used to derive N_{kt} values using standard or advanced laboratory test results. The statistical approach can often lead to higher N_{kt} values by forcing the in-situ data to fit standard test results on disturbed samples and consequently, lower, unrealistic, interpreted shear strengths.

The approach to evaluating undrained shear strength presented in this paper was developed using (1) in situ CPTu data and CPTu-based N_{kt} and (2) published NSP methods. The CPTu- and NSP-based approaches allow for the use of in situ data to converge on undrained shear strength values rather than

using standard laboratory testing to evaluate the N_{kt} and s_u. The two CPTu-based N_{kt} methods, presented by Mayne et al. [5] and Mayne and Peuchen [3], rely solely on the cone response to in situ conditions (point resistance and pore pressure) to evaluate N_{kt} and undrained shear strength. In contrast, the NSP methods presented by Quiros et al. [6] and Casey and Germaine [7] require soil stress history, index properties and advanced laboratory strength testing to evaluate undrained shear strength. The work presented here shows that, while the CPTu- and NSP-based N_{kt} methods approach the evaluation of undrained shear strength using different soil parameters (Figure 1), these five methods converge and lead to a more realistic, less conservative assessment of undrained shear strength.

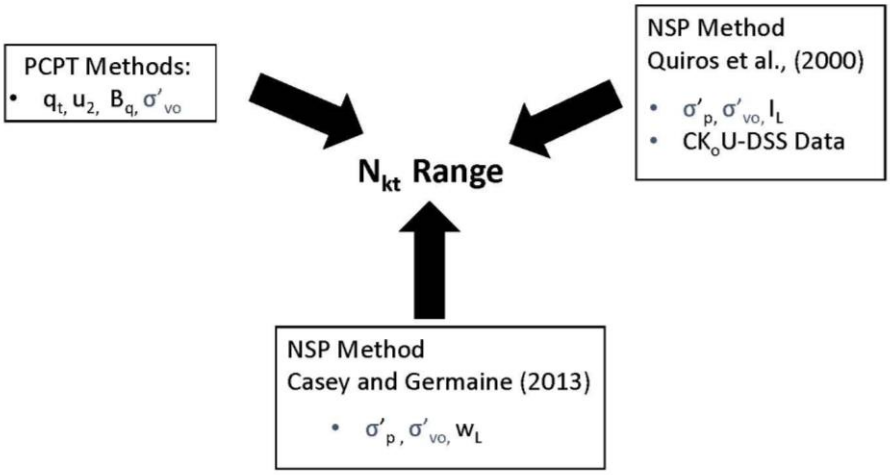

Figure 1. CPTu- and NSP-based methods.

2.1. CPTu-based N_{kt}

Although numerous studies have been conducted relating s_u to net cone resistance, q_{net}, the correlations presented in Mayne et al. [5] and Mayne and Peuchen [3] have been successfully used by the authors on numerous projects to evaluate CPTu-derived s_u. Mayne et al. [5] present an expression for N_{kt} as a function of normalized effective cone resistance, Q_U,

$$N_{kt} = 8.2\ Q_U^{0.3} \tag{2}$$

where $Q_U = (q_t\text{-}u_2)/\sigma'_{vo}$ and q_t is total cone resistance, u_2 is pore pressure, and σ'_{vo} is effective vertical overburden pressure.

Mayne and Peuchen [3] present the following equation as a function of CPTu pore pressure ratio, B_q:

$$N_{kt} = 10.5 - 4.6 * \ln(B_q + 0.1) \text{ with } B_q > -0.1 \tag{3}$$

where pore pressure ratio, $B_q = (u_2 - u_o)/q_{net}$, u_2 is pore pressure, u_o is hydrostatic pressure at the cone depth referenced to the seafloor and q_{net} is net cone resistance.

It is important to note that the benchmark shear strength test used to develop these two CPTu-based N_{kt} correlations is the K_o consolidated-undrained triaxial compression test (CAUC).

2.2. NSP methods

To assess the reasonableness of the s_u values derived from the two CPTu-based N_{kt} procedures described above, NSP methods were also used to evaluate the undrained shear strength. The SHANSEP (Stress History and Normalized Soil Engineering Parameter) method [9] has been used for many years to evaluate clay soils' normalized strength (s_u/σ'_{vc}) behavior. More recently, Quiros et al. [6] reported that consolidation pressure clearly had a significant effect on the s_u/σ'_{vc} ratio and CK_oU-DSS test results indicated a decrease in s_u/σ'_{vc} with increasing consolidation stress. Casey and Germaine [7] reported a similar effect of consolidation stress on shear strength ratio in CK_oU triaxial compression tests. Since the SHANSEP approach did not include this aspect of soil behavior, other SHANSEP-like NSP methods that accounted for the pressure effect on s_u/σ'_{vc} were selected to compare with the CPTu-based shear strengths.

The NSP methods presented by Quiros et al. [6] and Casey and Germaine [7] were selected to evaluate undrained shear strength. These methods require a well-defined stress history, soil index properties and, in the case of Quiros et al. [6], DSS-based laboratory test results to evaluate soil shear strength.

The Casey and Germaine method (C&G) is based on liquid limit, applied maximum stress, and is primarily derived from CK_oU triaxial compression tests. Undrained shear strength is expressed by the following equation:

$$s_{u,C} = \sigma'_{vo}\, S_1(\sigma'_P)^T(OCR^m) \tag{4}$$

where S_1 and T are functions of liquid limit ($S_1 = 0.0091w_{L[\%]} - 0.05$ and $T = -0.48\log_{10}(w_{L[\%]}) + 0.77$), σ'_{vo} is effective overburden pressure, σ'_P is applied maximum stress (or yield stress, σ'_y), OCR is overconsolidation ratio and m, the parameter relating OCR to normalized shear strength. An m value of 0.78 was used in this study based on our DSS database containing over 2500 tests with OCR = 1 and over 500 tests with OCR > 1. This m value compares well with the m value of 0.77 reported by Casey and Germaine [7].

The two NSP methods proposed by Quiros et al. [6], SP (Strength-Pressure) and SPW (Strength-Pressure-Water Content), are based on site-specific K_o-consolidated, undrained, strain-controlled, static direct simple shear (CK_oU-DSS) tests. The following equation can be used to evaluate undrained shear strength:

$$s_{u,D} = K_{sp}*(\sigma'_P{}^{\lambda_{sp}})(OCR^{m-1}) \tag{5}$$

where K_{sp} and λ_{sp} are the coefficient and exponent, respectively, in the SP correlation (c_u vs. σ'_{vc}) from a set of preferably site-specific DSS tests, and σ'_P, OCR and m are defined in the previous paragraphs. The original SPW correlation presented in Quiros et al. [6] has been recently modified to account for a soil's variation in plasticity. This modified relationship, SPLI, was used to compute the undrained shear strength and compare to CPTu-based values:

$$s_{u,D} = K_{SPLI}*(\sigma'_P/e^{LI})^{\lambda_{SPLI}}*(OCR^{m-1}) \tag{6}$$

where K_{SPLI} and λ_{SPLI} are, similarly, the coefficient and exponent, respectively, in the SPLI correlation (c_u vs. σ'_{vc}/e^{LI}) from a set of preferably site-specific DSS tests, LI is liquidity index (corrected to the LI the soil had at σ'_P if it has increased significantly due to stress relief) and σ'_P, OCR and m are as defined previously.

The reference shear strength tests for CPTu-derived shear strengths and the three NSP-derived strength strengths are advanced laboratory tests. The two CPTu-derived s_u and the Casey and

Germaine [7] equations (Equations 2, 3 and 4) are based on consolidated-undrained triaxial compression tests; CAUC and CK_oUC, or $s_{u,C}$. The two Quiros et al. [6] equations (Equations 5 and 6) are referenced to CK_oU-DSS tests, $s_{u,D.}$

Mayne and Peuchen [3] recommend the correlation, $s_{u,D} = 0.834 s_{u,C}$ (or $s_{u,C} = 1.2 s_{u,D}$), which can be used to relate the shear failure mode of the DSS test to the CAUC test. To confirm the relationship between $s_{u,D}$ and the $s_{u,C}$ proposed by Mayne and Peuchen [3], an $s_{u,D}$ database of over 2500 DSS tests (OCR = 1.0) were reviewed and an equivalent $s_{u,C}$ was evaluated using Casey and Germaine [7]. For these DSS tests conducted at a range of consolidation stresses ranging from about 20 kPa to about 9500 kPa, the average $s_{u,C}$ is approximately 1.185 times $s_{u,D}$, similar to the value of 1.2 proposed by Mayne and Peuchen [3]. A more detailed review of the DSS data indicated that, while the value of 1.185 works very well for the mid-range of consolidation stresses, a higher value is more appropriate at low stresses (e.g., $s_{u,C}/s_{u,D} = 1.3$ for 100 kPa) and a lower value is more appropriate at high stresses (e.g., $s_{u,C}/s_{u,D} = 1.0$ for 8,500 kPa). The relationship between $s_{u,D}$ and $s_{u,C}$ can be better defined over the tested range of consolidation stresses using the following relationships:

$$s_{u,C}/s_{u,D} = 1.749\ \sigma'^{-0.073}_{vc} \text{ for } 20 \leq \sigma'_{vc} \leq 192 \text{ kPa} \quad (7)$$

$$s_{u,C}/s_{u,D} = 1.245\ \sigma'^{-0.01}_{vc} \text{ for } 192 < \sigma'_{vc} \leq 4900 \text{ kPa} \quad (8)$$

$$s_{u,C}/s_{u,D} = 9.507\ \sigma'^{-0.248}_{vc} \text{ for } 4900 < \sigma'_{vc} \leq 9500 \text{ kPa} \quad (9)$$

where σ'_{vc} is σ'_P (or σ'_y) for underconsolidated, normally consolidated and overconsolidated clay.

3. Stress history

NSP methods for interpretation of undrained shear strength require a well-defined soil stress history. While consolidation tests can be used to estimate a soil's maximum previous consolidation pressure, σ'_P (or σ'_y), these tests can also be affected by sample disturbance. However, the data used from the sites in this study indicate that, in many cases, CRS (constant-rate-of-strain) tests can yield (a) reliable σ'_y values and (b) good agreement with CPTu-interpreted σ'_y.

Agaiby and Mayne [4] have reported the equation, $\sigma'_y = 0.33 q_{net}$, based on CPTu data to be the most reliable correlation to evaluate the σ'_y for most cohesive soils. This equation was used in this study to evaluate the yield stress ratio, YSR, defined as σ'_y/σ'_{vo} on soils ranging from underconsoldiated. Additionally, the term, apparent yield stress ratio (YSR*), relating yield stress and ***hydrostatic*** effective vertical pressure, $\sigma'_{vo,h}$, was adopted to allow values less than 1.0 to quantify the degree of underconsolidation of clays:

Therefore, $$YSR^* = 0.33 q_{net}/\sigma'_{vo,h} \quad (10)$$

4. Sites included in this study

Geotechnical data from seven sites were analyzed to develop N_{kt} correlations and evaluate s_u for a variety of fine-grained soils ranging from very underconsolidated to heavily overconsolidated clays. The seven sites represent marine soil deposits from around the world including offshore Africa, Asia, South America, and the Gulf of Mexico. Table 1 summarizes the soil properties and available geotechnical data for each location.

Table 1. Summary of sites used in correlation.

Site	Description	YSR*	Interpreted σ'_p Range, kPa	S_u Range, kPa	Index Tests	Boring Information Depth, m	Geotechnical Data
UC	Underconsolidated Clay (CH, CL)	0.8–0.3	5–740	1–225	$36 < w_L < 110$ $0.35 < I_L < 1.20$ $16 < I_P < 73$	147	PCPT, FV, UU, LV, CRS, DSS
NLOC	Normally to Lightly Overconsolidated Clay (CH, CL)	1.9–1.0	1–1135	1–335	$48 < w_L < 97$ $0.22 < I_L < 1.12$ $17 < I_P < 70$	121	PCPT, UU, LV, CRS, DSS
LOC	Lightly Overconsolidated Clay (CH)	2.4–1.4	35–1535	2–415	$50 < w_L < 80$ $0.19 < I_L < 1.30$ $29 < I_P < 54$	122	PCPT, UU, LV, CRS
MLOC1	Moderately to Lightly Overconsolidated Clay (CH)	3.5–1.6	15–1245	2–315	$96 < w_L < 166$ $0.32 < I_L < 0.99$ $49 < I_P < 129$	122	PCPT, UU, LV, CRS, DSS
MLOC2	Moderately to Lightly Overconsolidated Clay (CH)	5.8–2.4	40–700	5–165	$69 < w_L < 92$ $0.43 < I_L < 0.68$ $48 < I_P < 68$	44	PCPT, UU, LV, CRS
HOC	Heavily Overconsolidated Clay (CH), cemented	16–6	720–4950	75–920	$60 < w_L < 80$ $0.22 < I_L < -0.02$ $39 < I_P < 55$	82	PCPT, UU, LV, CRS, DSS
VHOC	Very Heavily Overconsolidated Clay (CH), cemented	27–11	865–10050	20–2015	$61 < w_L < 76$ $0.18 < I_L < -0.10$ $39 < I_P < 57$	81	PCPT, UU, LV, CRS, DSS

All seven sites have standard and advanced laboratory testing and in situ CPTu data. YSR* ($=0.33q_{net}/\sigma'_{vo,h}$) ranges from less than 1 (<0.3) in the UC soils to more than 25 in the VHOC soils with σ'_y up to 10,050 kPa. The consistency of the soils investigated range from very soft to very hard with undrained shear strengths up to 2015 kPa. The plasticity indices of the soils range between 16 and 73 with liquidity indices of 1.30 to less than zero.

It is noted in the table, and significant to this study, that the HOC and VHOC sites showed some indication of cementation. In the case of the VHOC site, the presence of an elevated ferrous content may explain the soils' natural cementation. This type of cementation, common in tropical clays, has been reported by Zhang et al. [10]. Application of the method proposed by Burland [11] to evaluate the in-situ state of the VHOC undisturbed soils and the influence of structure on soil properties also indicated a degree of cementation. Additionally, these were the only two sites where the UU triaxial compression strength measurements regularly exceeded the $s_{u,D}$ data.

5. Evaluations of N_{kt} factors

In this section, the authors first discuss the DSS-based N_{kt} envelope profiles, and then demonstrate how the resulting N_{kt} profiles compare in the first five sites (UC, NLOC, LOC, MLOC1, MLOC2). In these five sites, the standard laboratory strength tests generally compared well with the $s_{u,D}$ contours

yielded by the N_{kt} envelope profiles. Subsequently, the authors discuss the CAUC-based N_{kt} envelope profiles and show how the derived N_{kt} profiles compare in the two very overconsolidated clay sites (HOC, VHOC). Because of the hard to very hard consistency of the clays for these two sites and the presence of cementation, the UU triaxial compression test was the predominant standard laboratory strength test. Additionally, the UU triaxial tests did not demonstrate the same degree of disturbance as those in the other five sites. Consequently, as one would expect for UU triaxial tests performed on "ideally undisturbed" specimens, the tests at these two sites yielded strengths that agreed better with the $s_{u,C}$ contours yielded by the CAUC-based N_{kt} envelope profiles.

5.1. DSS-based N_{kt}

The two CPTu-based N_{kt} equations and the three NSP equations for undrained shear strength were used to evaluate the N_{kt} for each of the seven sites. To compare equivalent N_{kt} values derived from $s_{u,D\text{-}SP}$, $s_{u,D\text{-}SPLI}$ and $s_{u,C\text{-}C\&G}$, with those obtained from the CPTu-based methods (Equations 2 and 3), all N_{kt} were computed with $s_{u,D}$ as a reference using the following relationships:

$$\text{SP-based } N_{kt} = q_{net}/s_{u,D\text{-}SP} \tag{11}$$

$$\text{SPLI-based } N_{kt} = q_{net}/s_{u,D\text{-}SPLI} \tag{12}$$

$$\text{C\&G-based } N_{kt} = q_{net}/(s_{u,C\text{-}C\&G} \text{ converted to } s_{u,D\text{-}C\&G} \text{ using Equations 7, 8 and 9}) \tag{13}$$

As mentioned previously, the reference shear strength to develop the CPTu-based N_{kt} values obtained from Equations 2 and 3 from Mayne et al. [5] and Mayne and Peuchen [3] is the CAUC test. To compare equivalent CPTu-based N_{kt} values with the other three NSP-based N_{kt} values, the N_{kt} derived from Equations 2 and 3 were adjusted using Equations 7, 8 and 9 to obtain N_{kt} values relative to $s_{u,D}$. These $s_{u,D}$-based N_{kt} factors are denoted as $N_{kt,D}$.

Although N_{kt} values of 15 to 20 are often used by practitioners to interpret undrained shear strength in normally to moderately overconsolidated clays, N_{kt} varies with depth with a tendency to increase with increasing plasticity as well as to increase with decreasing sensitivity (Robertson and Cabal [12]). Rad and Lunne [13] indicated that N_{kt} factors can range from 8 to 29 with OCR being the principle variable.

The $N_{kt,D}$ values for the seven sites were calculated using the two CPTu-based equations and three NSP-based equations, and the YSR* was assessed using the ratio, $0.33q_{net}/\sigma'_{vo,h}$. Figures 2a and 2b present the $N_{kt,D}$ versus YSR* calculated by the five methods for the seven sites. The hydrostatic effective vertical stress ($\sigma'_{vo,h}$) profiles used to calculate YSR* are presented in the "a" graph of Figure 3 through 9 for the seven sites and include σ'_y interpreted from CPTu data and, in some cases, CRS tests.

The graph in Figure 2a includes a relatively tight band of N_{kt} versus YSR* for most of the data falling within the range of underconsolidated to lightly overconsolidated soils (YSR* $\leq$ 3.0). A deviation in the range of data occurs primarily with the HOC and VHOC soils with YSR* > 3.0, also shown in Figure 2b. These N_{kt} values falling outside most of the data were evaluated using the Mayne and Peuchen [3] method and are discussed in subsequent sections. To ascertain how each of the methods for the seven sites shown in Figures 2a and 2b compare, Figure 2b is presented again in the

appendix as Figure A1, while each of the five methods are presented separately in Figures A2 through A6.

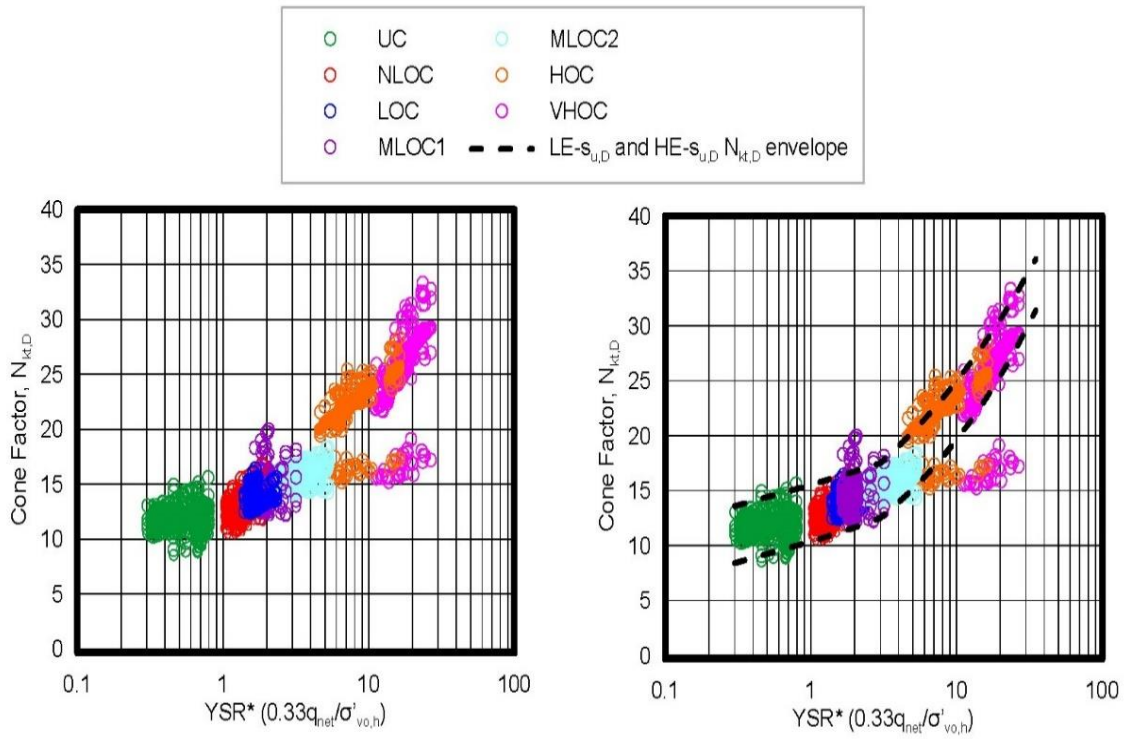

Figure 2a. $N_{kt,D}$ versus YSR* by location

Figure 2b. $N_{kt,D}$ versus YSR* with proposed LE-$s_{u,D}$ and HE-$s_{u,D}$ envelope

The $N_{kt,D}$ profiles are presented versus depth in the "b" graph of Figures 3 through 7 alongside the effective vertical stress graphs. For five of the seven sites (UC, NLOC, LOC, MLOC1 and MLOC2), the $N_{kt,D}$ versus depth profiles plot in a relatively narrow range.

Examination of Figures 2a and 2b reveal the following:

- $N_{kt,D}$ increases with increasing YSR* (or OCR for normally consolidated to overconsolidated clay).
- $N_{kt,D}$ values of about 10 to 15 are indicated for normally consolidated clay.
- For YSR* > 3, the $N_{kt,D}$ forms two branches as indicated by the $N_{kt,D}$ of the HOC and VHOC, which require consideration of the effects of cementation on undrained shear strength.
- A set of envelopes encompassing most of the data can be developed for Lower Estimate (LE)- and Higher Estimate (HE)-$s_{u,D}$ $N_{kt,D}$ for a quick evaluation of N_{kt} values based on the ratio, $q_{net}/\sigma'_{vo,h}$.

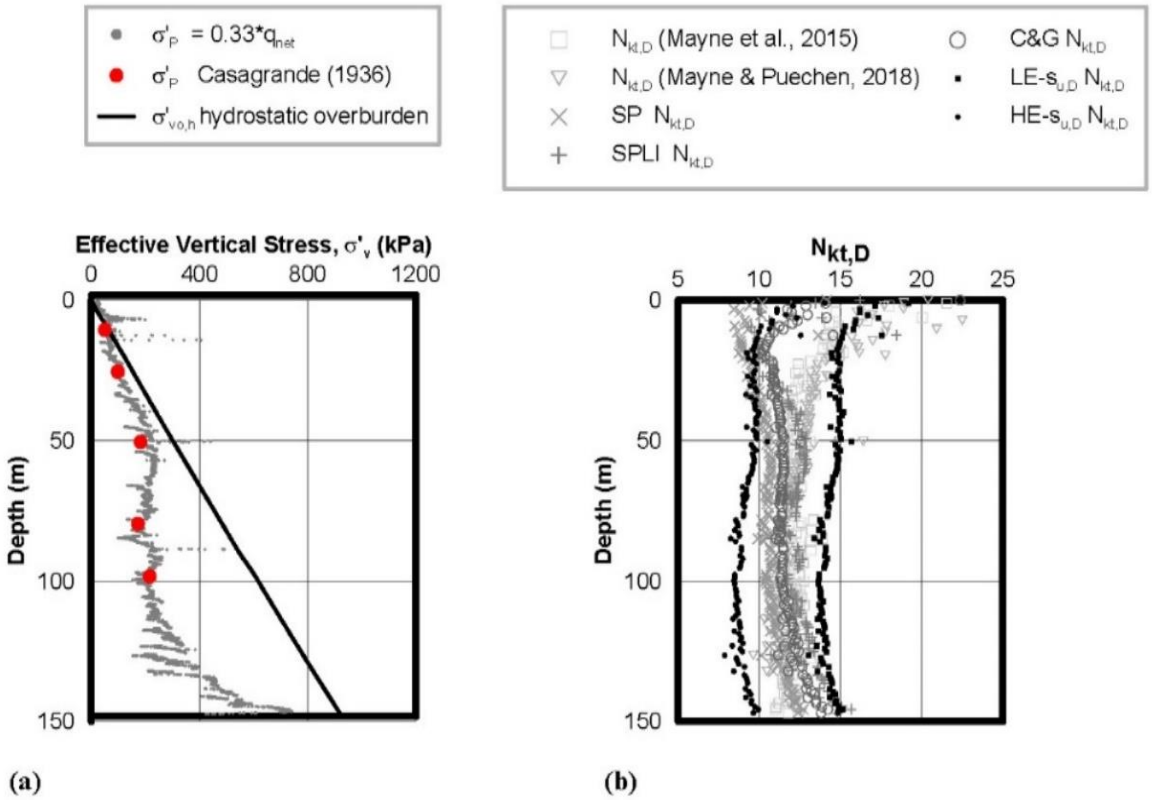

Figure 3. Underconsolidated (UC) Site: (a) effective vertical stress and (b) $N_{kt,D}$.

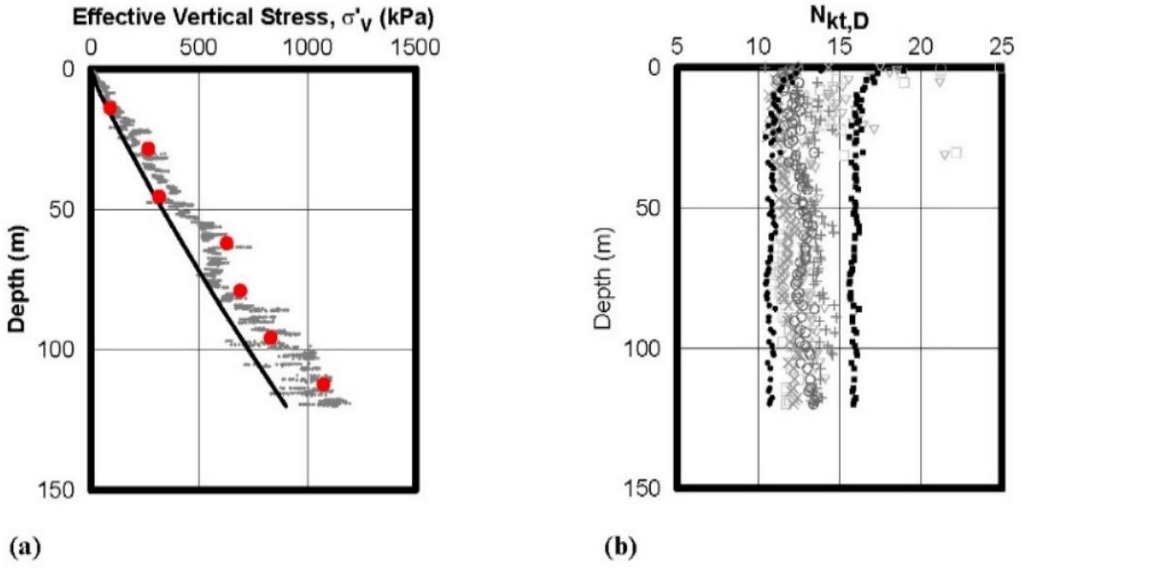

Figure 4. Normally to lightly overconsolidated (NLOC) Site: (a) effective vertical stress and (b) $N_{kt,D}$.

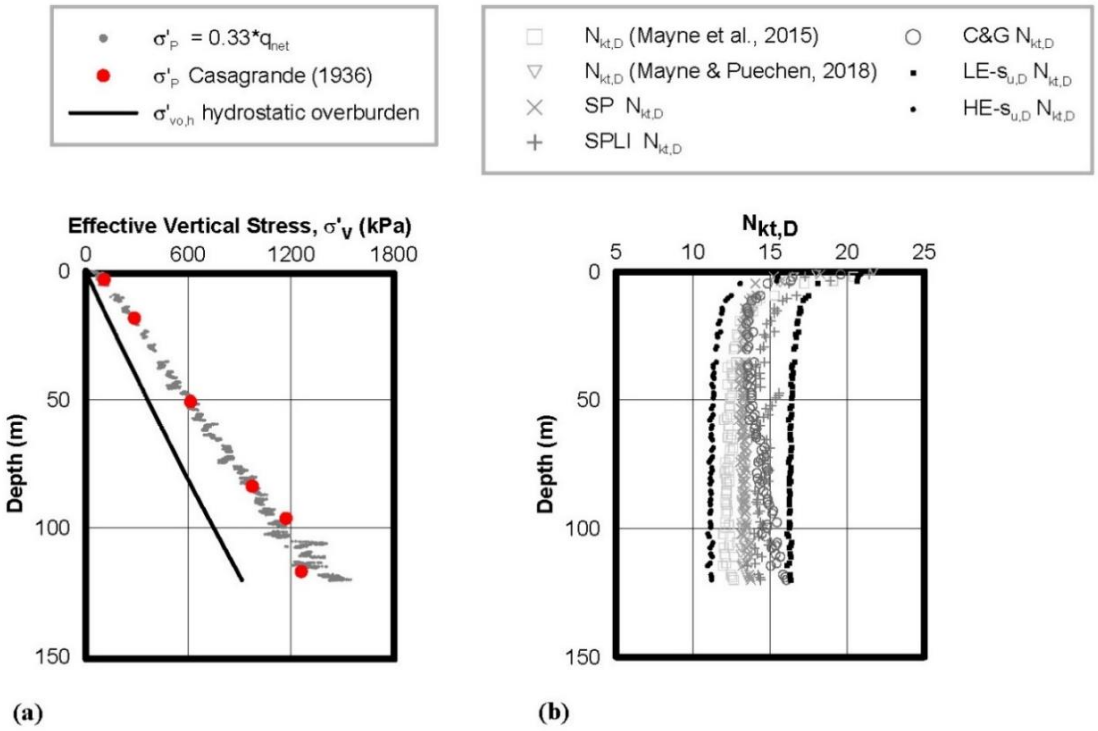

Figure 5. Lightly overconsolidated (LOC) Site: (a) effective vertical stress and (b) $N_{kt,D}$.

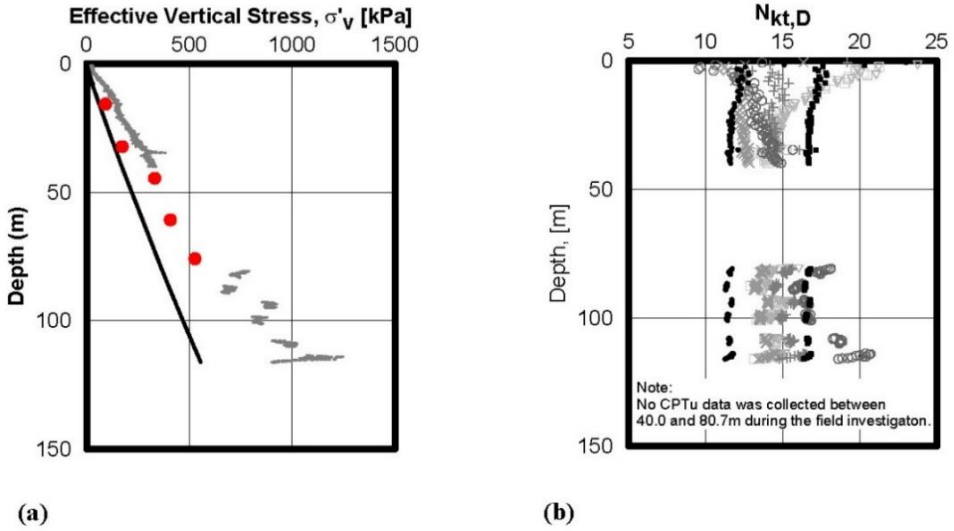

Figure 6. Moderately to lightly overconsolidated (MLOC1) Site: (a) effective vertical stress and (b) $N_{kt,D}$.

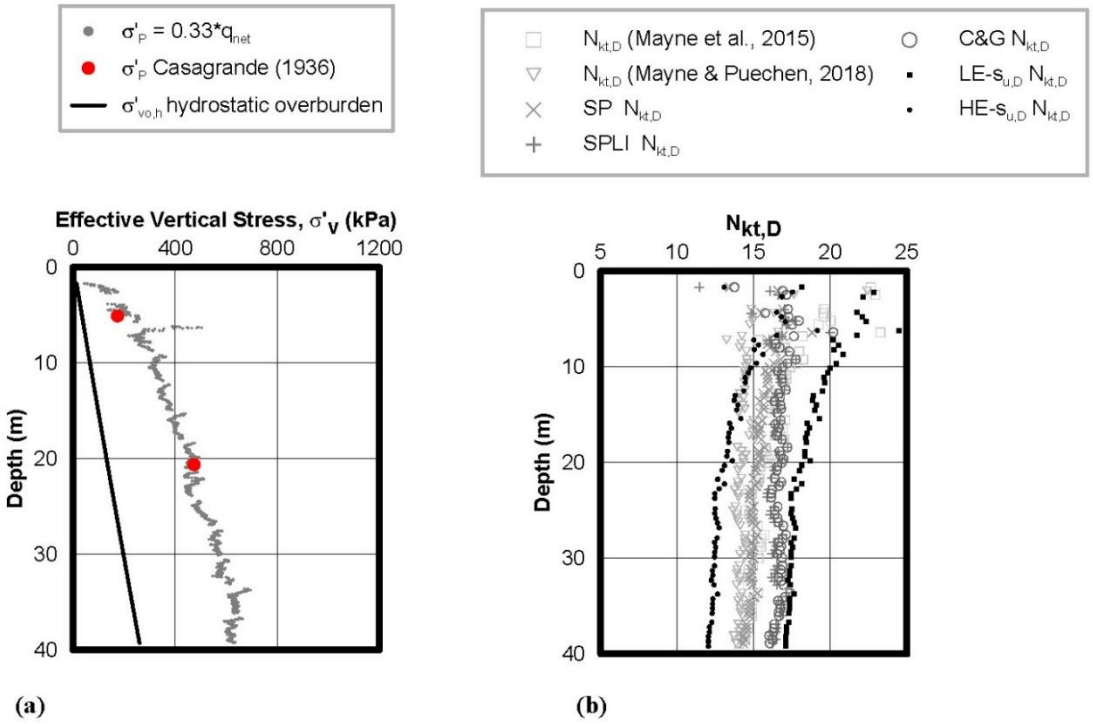

Figure 7. Moderately to lightly overconsolidated (MLOC2) Site: (a) effective vertical stress and (b) $N_{kt,D}$.

For soils that do not appear to be cemented, the following equations (indicated by dashed lines in Figure 2b) can be used to estimate LE- and HE-$s_{u,D}$ $N_{kt,D}$:

Lower Estimate-$s_{u,D}$ $N_{kt,D}$

$$\text{For YSR*} \leq 3.0,\ N_{kt,D} = 15.51(0.33q_{net}/\sigma'_{vo,h})^{0.11} \quad (14)$$

$$\text{For YSR*} > 3.0,\ N_{kt,D} = 12.67(0.33q_{net}/\sigma'_{vo,h})^{0.294} \quad (15)$$

Higher Estimate-$s_{u,D}$ $N_{kt,D}$

$$\text{For YSR*} \leq 3.0,\ N_{kt,D} = 10.34(0.33q_{net}/\sigma'_{vo,h})^{0.173} \quad (16)$$

$$\text{For YSR*} > 3.0,\ N_{kt,D} = 8.28(0.33q_{net}/\sigma'_{vo,h})^{0.375} \quad (17)$$

These envelopes were drawn to capture most of the data. The only data points that significantly deviate from the HE-$s_{u,D}$ $N_{kt,D}$ profile in Figure 2b correspond to the N_{kt} values evaluated using the Mayne and Peuchen [3] method (based on pore pressure ratio, B_q) for the HOC and VHOC soils with likely cementation.

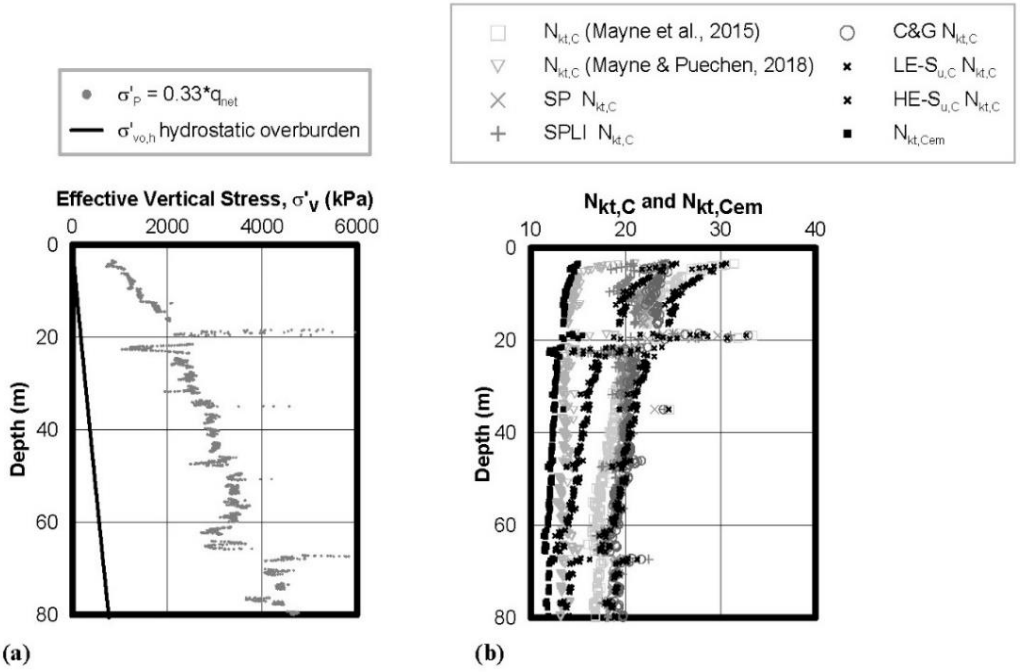

Figure 8. Heavily overconsolidated (HOC) Site: (a) effective vertical stress and (b) $N_{kt,C}$ and $N_{kt,Cem}$.

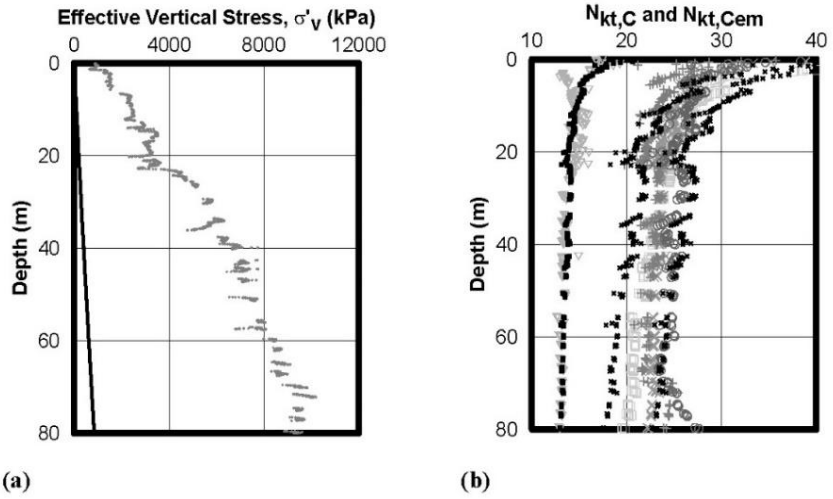

Figure 9. Very heavily overconsolidated (VHOC) Site: (a) effective vertical stress and (b) $N_{kt,C}$ and $N_{kt,Cem}$.

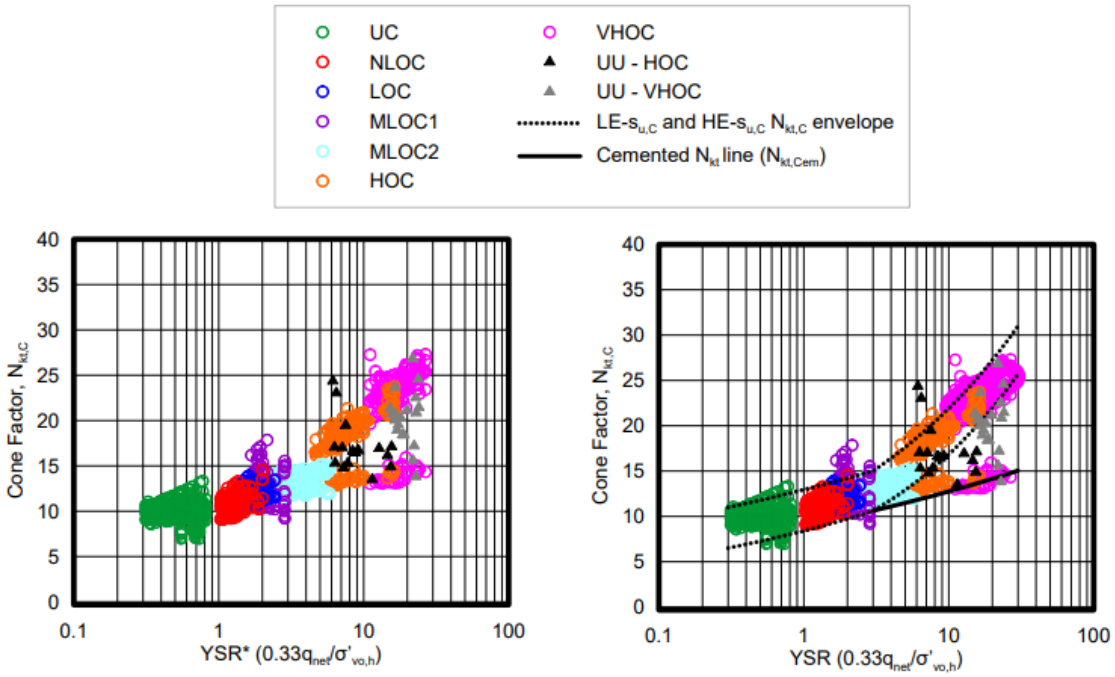

Figure 10a. $N_{kt,C}$ versus YSR* by location

Figure 10b. $N_{kt,C}$ and $N_{kt,Cem}$ versus YSR* with proposed LE-$s_{u,C}$ and HE-$s_{u,C}$ envelope and $N_{kt,Cem}$ profile

5.2. CAUC-based N_{kt}

The authors used a similar approach as discussed in the preceding section (*DSS-based N_{kt}*) to develop the CAUC-based N_{kt} envelope profiles. Since the two CPTu-based N_{kt} equations (Equations 2 and 3) and the C&G-derived N_{kt} (from Equation 4) are CAUC-based, these methods require no modification. However, the DSS-based SP and SPLI undrained shear strengths ($s_{u,D\text{-}SP}$, $s_{u,D\text{-}SPLI}$) were modified by multiplying these values by the pertinent factors derived from Equations 7, 8 and 9. The derived CAUC-based N_{kt} factor is denoted as $N_{kt,C}$. Figures 10a and 10b present the $N_{kt,C}$ versus YSR* calculated by the five methods for the seven sites. In Figure 10b, the CPTu-based $N_{kt,C}$ from Mayne et al. [5] and the three NSP-based $N_{kt,C}$ values plot within the dotted LE- and HE-$s_{u,C}$ $N_{kt,C}$ envelope. The CPTu-based $N_{kt,C}$ values derived from Mayne and Peuchen [3] fall within the dotted envelope up to a YSR* value of about 3. For YSR* > 3, this method deviates along the solid black line identified as $N_{kt,Cem}$ in Figure 10b. It is worthwhile to note that, in Figures 10a and 10b, the UU triaxial-based N_{kt} values for the HOC and VHOC sites plot mostly within the dotted $N_{kt,C}$ envelope as well as between the lower dotted $N_{kt,C}$ line and the $N_{kt,Cem}$ line. This behavior is likely due to variation in degrees of cementation in the soil deposit. For comparison purposes, Figure 10b is presented again in the appendix as Figure A7 while each of the five methods are presented separately in Figures A8 through A12. In appendix Figure A13, we also present the UU triaxial test results for the HOC and VHOC sites for clearer visualization.

For uncemented, fine-grained cohesive sediments, the following equations can be used to define the dotted lines in Figure 10b:

Lower Estimate-$s_{u,C}$ $N_{kt,C}$

$$\text{For YSR*} \leq 3.0,\ N_{kt,C} = 12.94(0.33q_{net}/\sigma'_{vo,h})^{0.135} \quad (18)$$

$$\text{For YSR*} > 3.0,\ N_{kt,C} = 10.61(0.33q_{net}/\sigma'_{vo,h})^{0.315} \quad (19)$$

Higher Estimate-$s_{u,c}$ $N_{kt,C}$

$$\text{For YSR*} \leq 3.0,\ N_{kt,C} = 8.4(0.33q_{net}/\sigma'_{vo,h})^{0.212} \quad (20)$$

$$\text{For YSR*} > 3.0,\ N_{kt,C} = 6.94(0.33q_{net}/\sigma'_{vo,h})^{0.385} \quad (21)$$

For clayey soils with a YSR* > 3 that may be cemented, the following equation can be used to develop an N_{kt} profile that yields an upper bound undrained shear strength profile ($s_{u,Cem}$):

$$\text{For YSR*} > 3.0,\ N_{kt,Cem} = 9(0.33q_{net}/\sigma'_{vo,h})^{0.151} \quad (22)$$

Using Equations 18 through 22, LE- and HE-$s_{u,C}$ $N_{kt,C}$ and $N_{kt,Cem}$ profiles were developed for the HOC and VHOC sites. The $N_{kt,C}$ profiles calculated by the five methods are presented in the "b" graph of Figures 8 and 9. These figures also contain the LE- and HE-$s_{u,C}$ $N_{kt,C}$ and $N_{kt,Cem}$ profiles. The reader can observe in Figures 8b and 9b that the three NSP-based $N_{kt,C}$ data and the Mayne et al. [5] CPTu-based $N_{kt,C}$ values fall within the LE- and HE-$s_{u,C}$ $N_{kt,C}$ envelope. Alternatively, the Mayne and Peuchen [3] CPTu-based $N_{kt,C}$ data nicely track the $N_{kt.Cem}$ profile.

6. Evaluation of s_u

As discussed previously, standard laboratory shear strength measurements can vary considerably depending on sample disturbance due to stress relief, gas exsolution and sample expansion, silt and sand inclusions, etc. Lunne et al. [14] suggest that tube sampling strains can also add to diminished sample quality. However, the undrained shear strength assessed by combining the CPTu and NSP methods recommended in this paper can converge on a more consistent, reasonable, and less conservative shear strength interpretation.

Figures 11 through 14 (UC, NLOC, LOC, MLOC1) present standard laboratory shear strength measurements along with the shear strength profiles interpreted from the in situ CPTu data using the LE- and HE-$s_{u,D}$ envelope shown in Figure 2b. For the MLOC2 site in Figure 15, the standard laboratory strength data are presented along with the LE- and HE-$s_{u,D}$ envelope from Figure 2b, and the LE- and HE-$s_{u,C}$ envelope from Figure 10b.

The undrained shear strength profiles for the UC site are shown in Figure 11. The LE-$s_{u,D}$ and HE-$s_{u,D}$, profiles agree well with the lab vane (LV) and UU triaxial shear strengths in the upper 40 meters. Below 40 m, many of the LV and UU tests affected by stress relief, gas expansion and the associated disturbance, fall below the LE-$s_{u,D}$ profile, particularly between 40 and 90 meters. Below 90 m, while some of the LV and UU laboratory tests fall below the LE-$s_{u,D}$ profile, many of the UU tests plot within the LE- and HE-$s_{u,D}$ range, lending confidence in an interpreted shear strength profile using the CPTu-based LE- and HE-$s_{u,D}$ profiles and not the standard laboratory tests on acquired samples.

Similar trends in the laboratory and in situ undrained shear strength data and profiles are seen in Figures 12 through 14 for the NLOC, LOC and MLOC1 sites. The measured laboratory shear strength measurements in the upper 40 to 50 m at these sites fall within the LE- and HE-$s_{u,D}$ envelope indicating better sample quality and less disturbance. Below 40 to 50 m, many of the laboratory strength measurements fall at or below the LE-$s_{u,D}$ profile.

Figures 11 through 14 illustrate that the standard testing at shallower penetrations (less than 40 to 50 m) does not exhibit the same degree of sample disturbance as samples acquired at deeper

penetrations. This trend is also observed in Figure 15 for the MLOC2 site where UU laboratory data plot well within the LE- and HE-$s_{u,D}$ envelope and coincide with the LE-$s_{u,C}$ profile.

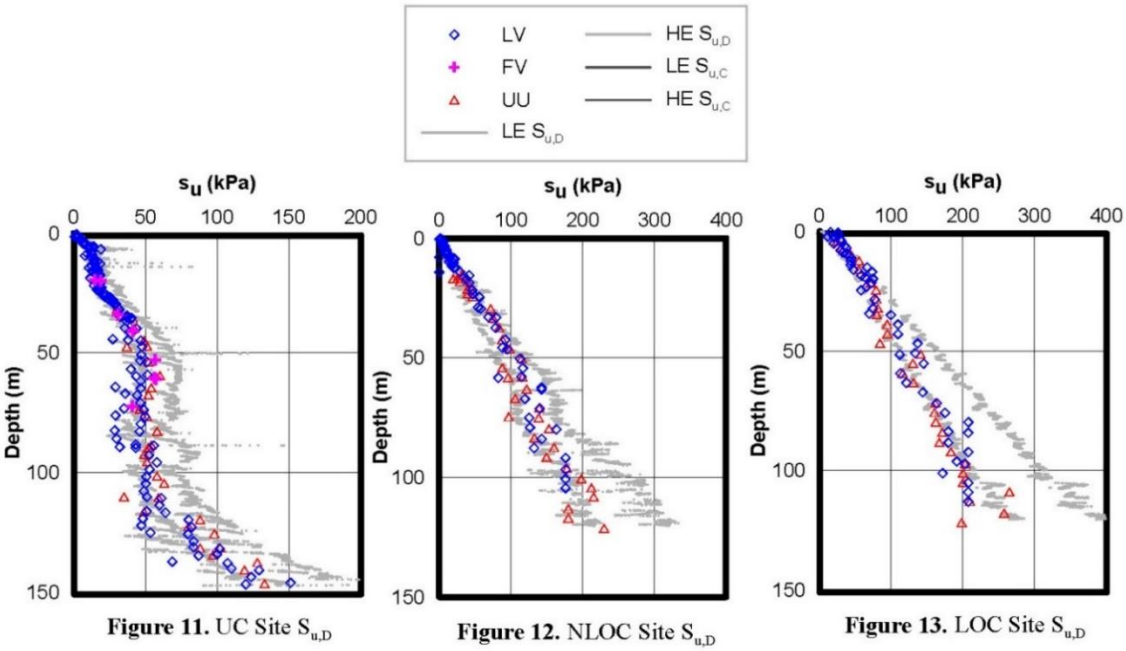

Figure 11. UC Site $S_{u,D}$

Figure 12. NLOC Site $S_{u,D}$

Figure 13. LOC Site $S_{u,D}$

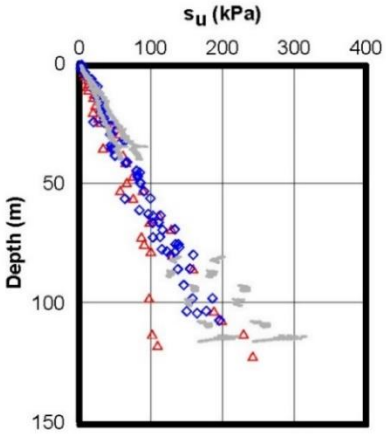

Figure 14. MLOC1 Site $S_{u,D}$

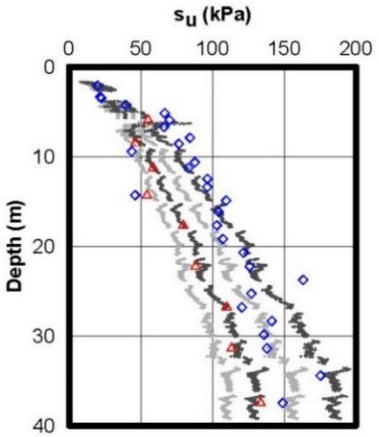

Figure 15. MLOC2 Site $S_{u,D}$ and $S_{u,C}$

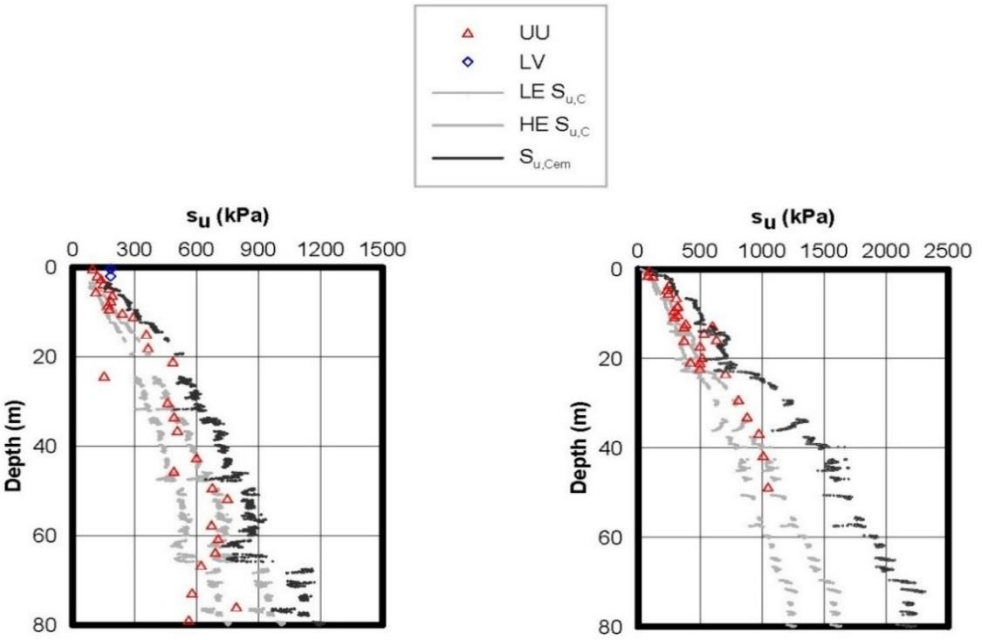

Figure 16. HOC Site $S_{u,C}$ and $S_{u,Cem}$

Figure 17. VHOC Site $S_{u,C}$ and $S_{u,Cem}$

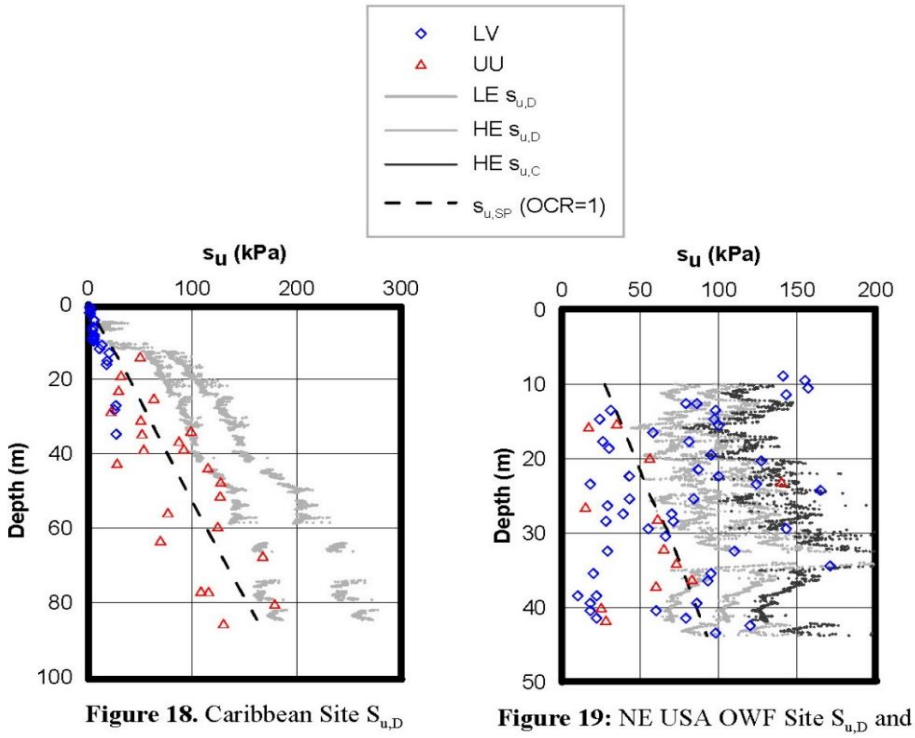

Figure 18. Caribbean Site $S_{u,D}$

Figure 19: NE USA OWF Site $S_{u,D}$ and $S_{u,C}$

Figures 16 and 17 present the laboratory strength tests, the LE- and HE-$s_{u,C}$ trendlines and the $s_{u,Cem}$ profile for the HOC and VHOC sites. Because of the hard consistency of the clay at these two sites, most of the standard laboratory strength tests consist of UU triaxial tests. These two graphs illustrate that, at shallow penetrations less than about 20 m, the standard laboratory s_u measurements fall between the HE-$s_{u,C}$ and the $s_{u,Cem}$ profiles. Below 20-m depth, most of the UU triaxial measurements plot along the HE-$s_{u,C}$ profile, with a few falling within the LE- and HE-$s_{u,C}$ envelope. Interestingly, for skin friction calculations of driven piles at the VHOC site, the project team assumed that cementation of the soil would be broken up by the driving process and, for this reason, selected the LE-$s_{u,C}$ profile for the undrained shear strength. A pile drivability study that included pile monitoring was conducted for this site, and it confirmed the validity of this approach [15].

7. Proposed procedure applied to other sites

While the CPTu- and NSP-based N_{kt} approach presented here was successfully applied to the seven sites selected for this study, additional sites were also analyzed to check the applicability of the method. Figure 18 presents data for a clay site in the Caribbean, including LV and UU data along with the LE- and HE-$s_{u,D}$ profiles computed using the corresponding $N_{kt,D}$ envelope. To assist in evaluating the disturbance of the LV and UU laboratory tests, a lower bound $s_{u,D}$ profile based on a normally consolidated SP method, $s_{u,SP}$ (OCR = 1), is also shown as a dashed line. Below 12 m, many of the UU tests are below the $s_{u,SP}$ (OCR = 1) line, with a few UU tests plotting on the LE-$s_{u,D}$ profile. A shear strength profile following the LE-$s_{u,D}$ trend can be selected with confidence, despite the variability in the standard laboratory strength data, particularly because the laboratory consolidation tests and CPTu soundings clearly indicated that these sediments were lightly overconsolidated. Similarly, a northeast USA windfarm site was analyzed. The standard laboratory s_u data, the $s_{u,SP}$ (OCR = 1) line, as well as the LE- and HE-$s_{u,D}$ and the HE-$s_{u,C}$ profiles are presented in Figure 19. The laboratory LV and UU data are widely scattered, in part due to the many silt and sand inclusions in the recovered samples. The $s_{u,SP}$ (OCR = 1) profile helps evaluate the disturbance in the laboratory tests, and the LE-$s_{u,D}$, the HE-$s_{u,D}$ and the HE-$s_{u,C}$ profiles can aid in selection of a design shear strength in this moderately to lightly overconsolidated soil deposit.

This proposed NSP-CPTu procedure for estimating N_{kt} was also applied to 22 published sites from around the world listed in Table 2. In addition to presenting "normal clay" sites, the table contains sites of sensitive clays from the USA, Canada, Norway, and Finland; clayey carbonate mud in offshore Indonesia; and the organic Sarapuí clay in Brazil. Additionally, the list contains a highly plastic clay site in West Africa, two silt stratigraphy sites in Norway, as well as the well-documented Bothkennar clay in the UK and the Boston Blue clay in the northeastern USA. Also included is a glacial till in the UK and another glacial till in Sweden. The right-hand column of the table describes how the s_u profiles generated from the proposed NSP-CPTu procedure for estimating N_{kt} compared with data presented in specific figures of the cited publications. The data presented in the published papers varied from field vanes (FV) to dilatometer (DMT)-based s_u as well as DSS-based and CAUC-based s_u. A careful review of the results presented in Table 2 demonstrates that the proposed procedure yielded results that agreed remarkably well with data from the published sites.

Table 2. Application to published sites.

Location	Soil Type	Reference	Method application result (Cited figures are in reference paper)
LUVA site (Aasta Hansteen), Norwegian Sea	Lightly overconsolidated clay	Lunne et al. [14]	*Fig. 2*: s_u for N_{kt} = 12 is tightly enclosed by the LE- & HE-$s_{u,D}$ envelope to 8-m depth; below 8 m, it coincides with the average of the LE- & HE-$s_{u,D}$ envelope. The s_u for N_{Ball} = 9.5 is tightly enclosed by the LE- & HE-$s_{u,C}$ envelope to 8-m depth; below 8 m, it falls between the average of the LE- & HE-$s_{u,C}$ envelope and the LE-$s_{u,C}$ profile. In Fig. 10, most corrected CAUC are tightly enclosed by the average of the LE- & HE-$s_{u,C}$ envelope and the LE-$s_{u,C}$ profile.
Tiller-Flotten site, Norway	Lightly overconsolidated clay (Sensitive clay below 7.5m)	L'Heureux et al. [16]	*Fig. 25*: The CAUC on block samples fall along the HE-$s_{u,C}$ profile. The dilatometer (DMT)-based $s_{u,C}$ data fall slightly below the HE- $s_{u,C}$ profile except between 14 to 16 m where they fall just above the LE-$s_{u,C}$ profile.
Onsøy site, Norway	Lightly overconsolidated clay	Gundersen et al. [17]	*Fig. 16*: The Best Estimate DSS profile for the site falls along the LE-$s_{u,D}$ profile to 14 m & along the average of the LE- & HE-$s_{u,D}$ envelope below 14 m. The Best Estimate CAUC profile for the site falls close to the average of the LE- & HE-$s_{u,C}$ envelope.
Dragvoll site, Norway	Lightly overconsolidated, low plasticity, highly sensitive glaciomarine clay	Helle et al. [18]	*Fig. 4d*: The CPTu-based $s_{u,Nkt}$ & $s_{u,N\Delta u}$ profiles and the SHANSEP-based s_u profile fall slightly below the HE-$s_{u,C}$ profile. The CAUC fall along the HE-$s_{u,C}$ profile.
Halden site, Norway	Lightly overconsolidated silt	Blaker et al. [19]	*Fig. 26a*: The CPTu-based s_u profiles for N_{kt} = 15 & 18 are tightly enclosed within the LE- & HE-$s_{u,D}$ envelope. The CAUC tests fall on or slightly above the LE-$s_{u,C}$ profile.
Halsen-Stjordal site, Norway	Lightly overconsolidated silt	Bihs et al. [20]	*Fig. 16*: Six of seven CAUC tests based on the more consistent failure criteria 2 & 5 are tightly enclosed by the LE- & HE-$s_{u,C}$ envelope.
Tornhill glacial till, Sweden	Heavily overconsolidated clay till	Larsson [21]	*Fig. 2*: If upper and lower profiles are drawn of the tip resistance (q_T) profiles presented on the left graph of Fig. 2, employing the $N_{kt,cem}$ equation to the derived q_{net} profiles yields upper and lower $s_{u,Cem}$ profiles that nicely envelope the core of the field vane-based undrained shear strength profiles presented on the right graph of Fig. 2.
Perniö site, Finland	Lightly overconsolidated, very sensitive clay (S_t = 40 to 60)	Di Buò et al. [22]	*Fig.11a*: 9 of 11 CIUC/CAUC, & associated N_{kt}-, N_{du}-, & N_{ke}-based s_u profiles fall on or slightly below the HE-$s_{u,C}$ profile. *Fig. 11b*: Most of the DSS & field vane, & associated N_{kt}-, N_{du}-, & N_{ke} based s_u profiles fall on or slightly above the LE-$s_{u,D}$ profile.

Continued on next page

Location	Soil Type	Reference	Method application result (Cited figures are in reference paper)
Bothkennar site, UK	Lightly overconsolidated, clay	Nash et al. [23]	*Fig.11a*: 15 of 17 UU triaxials on piston samples are tightly enclosed by the LE- & HE-$s_{u,D}$ envelope; UU triaxials on Laval samples are tightly enclosed by the LE- & HE-$s_{u,C}$ envelope. *Fig. 11b*: Field vanes generally lie along the average of the LE- & HE-$s_{u,C}$ envelope. *Fig. 11c:* Most of the self-boring pressuremeter (SBPM) are tightly enclosed by the LE- & HE-$s_{u,C}$ envelope, while the DMT profile falls on the LE-$s_{u,C}$ profile.
Cowden glacial till, UK	Heavily overconsolidated clay till	Zdravcović et al. [24]	*Fig. 11(a):* The interpreted $s_{U,TXC}$ profile essentially falls between the $s_{u,Cem}$ and the non-cemented HE-$s_{u,C}$ profiles from 0-m to 5.5-m depth and within the non-cemented LE- & HE-$s_{u,C}$ envelope below 5.5 m. *Fig. 11(b):* The CPT-derived s_u (N_{kt}=16) profile essentially falls between the $s_{u,Cem}$ and the non-cemented HE-$s_{u,C}$ profiles from 0 to 5.5 m, and within the non-cemented LE- & HE-$s_{u,C}$ envelope below 5.5 m.
AMU Morasko clay site, Poland	Lightly to moderately overconsolidated clayey silty sand to sandy clay	Radaszewski & Wierzbicki [25]	*Fig. 21*: The DMT- & CPTu-based (N_{kt} = 13/15) s_u profiles are tightly enclosed by the LE- & HE-$s_{u,D}$ envelope.
Leda clay, eastern Canada	Lightly overconsolidated clay (Sensitive clay)	Mayne et al, [26]	*Fig. 18*: Most of the field-vane, CPTu-, CIUC- and CAUC-based s_u data are tightly enclosed within the LE- & HE-$s_{u,C}$ envelope.
Port of Ploce, Croatia	Normally to lightly overconsolidated clay	Kavur et al. [27]	*Fig. 4a*: The s_u based on CPTu (N_{kt} = 14), DMT & field vane are tightly enclosed within the LE- $s_{u,D}$ profile and the average of the LE- & HE-$s_{u,D}$ envelope.
Presumpscot clay Dover, New Hampshire, USA	Normally to lightly overconsolidated sensitive clay	Mayne & Benoît [28]	*Fig. 13(a)*: The CPT-derived $s_{u,C}$ (N_{kt} = 11.3) profile falls just above the LE $s_{u,C}$ profile at shallow depth and increases to midrange of the LE- & HE-$s_{u,C}$ envelope with depth. *Fig. 13(b)*: The S_{UV} data track the LE $s_{u,D}$ profile.
Newbury, Massachusetts, USA	Lightly to moderately overconsolidated clay	DeGroot et al. [29]	*Fig. 20a*: The CPTu- & DSS-based s_u data are tightly enclosed within the average of the LE- & HE-$s_{u,D}$ envelope and the LE- $s_{u,D}$ profile. The CAUC are tightly enclosed within the LE- & HE-$s_{u,C}$ envelope.
Mad Dog, Deepwater Gulf of Mexico, USA	Normally to heavily overconsolidated clay	Liedtke et al. [30] Schroder et al. [31]	*Figs. 3b & 3d*: The s_u for N_{kt} = 16 is tightly enclosed within the LE- & HE $s_{u,D}$ envelope.
Mekong Delta, west coast of southern Vietnam	Normally to lightly overconsolidated clay	Giao et al. [32]	*Fig. 7*: Field vane-based s_u data (adjusted as per Aas et al., 1986), between 2-m & 16-m depths, fall within the LE- & HE- $s_{u,D}$ envelope.

Continued on next page

Location	Soil Type	Reference	Method application result (Cited figures are in reference paper)
Gulf of Guinea, West Africa	Lightly overconsolidated, highly plastic clay	Ozkul et al. [33]	*Figs. 4a and 4b*: The s_u data based on CPTu and recompression DSS, for two sites, are tightly enclosed by the LE- & HE- $s_{u,D}$ envelope.
Timor Sea, Indonesia	Siliceous clayey carbonate mud, lightly overconsolidated	Trevor et al. [34]	*Figs. 14 & 15:* s_u for N_{kt} = 15 falls at to slightly above the LE-$s_{u,D}$ profile. Other laboratory test s_u values are higher but tightly enclosed within the LE- & HE- $s_{u,D}$ envelope.
Sarapui clay, Brazil	Lightly overconsolidated, organic clay	Danziger et al. [35]	*Fig. 14*: Below 2m, most of the Jannuzzi (2009) field vane tests and the seismic dilatometer tests (SDMT) are tightly enclosed within the LE- & HE-$s_{u,C}$ envelope.
Ballina clay, Australia	Lightly overconsolidated clay	Pineda et al. [36]	*Fig, 13a*: Below 2-m depth, 18 of 21 triaxial compression tests are tightly enclosed within the LE- & HE-$s_{u,C}$ envelope. *Fig. 13b*: Below 2-m depth, all field vane tests, the SDMT profile & the CPTu-based s_u (N_{kt} = 13.2) profile are tightly enclosed within the LE- & HE-$s_{u,D}$ envelope.
Burswood clay, Australia	Lightly overconsolidated clay	Low et al. [37]	*Fig. 17a*: The CPTu-based s_u (N_{kt} = 10), the DSS-based s_u on tube & block samples, & the triaxial compression-based s_u on tube & block samples are tightly enclosed within the LE- & HE- $s_{u,C}$ envelope. Most of the DSS based s_u data fall along the HE-$s_{u,D}$ profile, which is about in the center of the LE- & HE-$s_{u,C}$ envelope.

8. How to use the NSP-CPTu procedure

To employ the proposed procedure for a fine-grained sediment stratum requires: (a) site-specific CPTu data and (b) the hydrostatic effective vertical stress, $\sigma'_{vo,h}$, of the stratigraphy. For *underconsolidated* sediments where the stratigraphy has not reached a hydrostatic effective stress state, in the term $q_{net}/\sigma'_{vo,h}$, the denominator refers to the *potential* hydrostatic vertical effective stress for that underconsolidated stratigraphy. Additionally, the authors presented the N_{kt}-$0.33q_{net}/\sigma'_{vo,h}$ correlation equations (14 through 22) because graphing the CPTu data in this fashion would give the user a *sense* of the stress history of the stratigraphy being analyzed. However, if preferred, the user can rewrite these equations and simply use the N_{kt}-$q_{net}/\sigma'_{vo,h}$ correlations without the "0.33" term. These re-formulated equations are presented in the appendix in Table A1.

The steps for using the NSP-CPTu procedure are as follows:

1. Generate the q_{net} profile for the stratigraphy being analyzed from the CPTu data. Also generate its ***hydrostatic*** effective vertical stress profile, $\sigma'_{vo,h}$.
2. Use Equations 14 through 17 or Equations 18 through 22, as appropriate, to generate the LE-$s_{u,D}$ and HE-$s_{u,D}$ $N_{kt,D}$ profiles versus depth, or the LE-$s_{u,C}$ and HE-$s_{u,C}$ $N_{kt,C}$ and $N_{kt,Cem}$ profiles.
3. Use the generated N_{kt} profiles from Step 2 in conjunction with the q_{net} profile to develop the corresponding s_u profiles (LE $s_{u,D}$, HE $s_{u,D}$, LE $s_{u,C}$, HE $s_{u,C}$, $s_{u,Cem}$). Insert these profiles in a graph with all other s_u data measurements to evaluate the undrained shear strength for the study site.
4. The s_u data for a particular site could fall on the LE-s_u profile, or on the HE-s_u profile, or in between the two profiles, whether they be $s_{u,D}$-based or $s_{u,C}$-based. The LE and HE envelope is only

giving bounds as to where site-specific s_u data should likely be. **Generally, standard laboratory s_u data that plot significantly below a site-specific LE $s_{u,D}$ profile are likely disturbed**. It is worthwhile to note the LE- and HE-$s_{u,D}$ envelope and the LE- and HE-$s_{u,C}$ envelope overlap. This characteristic was also observed in several of the published sites listed in Table 2 (as example, see Figure 15).

5. In offshore foundation design practice, the norm is to interpret design s_u profiles based on good quality UU triaxial compression tests. However, as discussed earlier, for clays with OCR < 3, these standard laboratory strength tests may be more susceptible to sample disburbance below about 30- to 50-meter sampling depth. Since undisturbed UU triaxial tests on 76-mm-OD thin-walled tube samples for these clays typically fall within the LE-and HE-$s_{u,D}$ envelope, we recommend interpreting a design s_u profile equivalent to at least the LE-$s_{u,D}$ profile when the UU triaxial measurements are below that profile.

6. If the OCR values for a specific site exceed 3 and its UU triaxial compression tests exceed the HE-$s_{u,D}$ profile, this is likely an indication that the cemented-soil equation (Equation 22) should be considered in conjunction with the other equations (Equations 20 and 21) for uncemented clay when evaluating the undrained shear strength.

9. Conclusions

The authors have proposed a procedure for selecting N_{kt} values to use with CPTu data for interpreting undrained shear strength. They developed the NSP-CPTu procedure by analyzing data from seven cohesive fine-grained sediment sites that ranged from moderately plastic to highly plastic, and that had stress histories ranging from underconsolidated to very heavily overconsolidated. The analyses for the proposed procedure incorporated the results from two published CPTu-based methods for N_{kt} interpretation, and three NSP-based methods for s_u interpretation that were converted to equivalent N_{kt} profiles. It was found that the resulting N_{kt} profiles from these analyses fell within a relatively narrow range that could be bound with a series of equations relating N_{kt} to the term, $q_{net}/\sigma'_{vo,h}$. The procedure yields very reasonable undrained shear strength interpretations for a variety of fine-grained soil types. The NSP-CPTu method has been shown to be superior to the approach of simply correlating q_{net} to standard laboratory undrained shear strength tests. These standard tests can be unavoidably disturbed due to the sampling process, thus leading to unduly conservative undrained shear strength interpretations. An advantage to this method is that it provides a CPTu-based undisturbed undrained shear strength that can be used as a baseline to help assess the sensitivity and thixotropy and the degree of disturbance of other laboratory tests. The underconsolidated UC and heavily overconsolidated sites presented in Table 1 and the highly sensitive Dragvoll and Leda sites presented in Table 2 indicate that this NSP-CPTu method yields very reasonable assessments of undrained shear strength for a wide variety of soil types. Additionally, this study has shown that (1) N_{kt} is not necessarily constant with depth and has been found to vary with the ratio, $q_{net}/\sigma'_{vo,h}$; and (2) the practice of limiting N_{kt} to a range of only 15 to 20 for normally consolidated to lightly overconsolidated clays seems unjustified.

In addition to employing the NSP-CPTu procedure in standard practice, it can be particularly valuable in interpreting undrained shear strength in areas where CPTu soundings are performed but in which there is very little geotechnical experience.

Acknowledgement

The authors would like to thank Fugro USA Marine, Inc., for facilitating the preparation of this paper.

Notation

The following symbols are used in this paper:

$\sigma'_{vo,h}$ = hydrostatic effective vertical stress

σ'_{vo} = effective vertical stress

σ'_{vc} = vertical consolidation pressure

σ'_{y} or σ'_{p} = maximum preconsolidation pressure

s_u or c_u = undrained shear strength

$s_{u,D}$ = undrained shear strength based on K_o-consolidated, undrained, strain-controlled, static direct simple shear (CK_oU-DSS) tests

$s_{u,C}$ = undrained shear strength based on consolidated-undrained triaxial compression tests; CAUC and CK_oUC

$s_{u,D\text{-}SP}$ = undrained shear strength based on Quiros et al. [6], SP (Strength-Pressure) method

$s_{u,D\text{-}SPLI}$ = undrained shear strength based on Quiros et al. [6], SPW (Strength-Pressure-Water Content) method, modified using liquidity index in lieu of water content

$s_{u,C\text{-}C\&G}$ = undrained shear strength based on Casey & Germaine [7] method

w_L = liquid limit

I_p = plasticity index

I_L = liquidity index

Conflict of interest

All authors declare no conflicts of interest in this paper.

References

1. Young AG, Quiros GW, Ehlers CJ (1983) Effects of offshore sampling and testing on undrained soil shear strength. *Annu Offshore Technol Conf*. Houston, Texas, USA. https://doi.org/10.4043/4465-MS
2. Quiros GW, Young AG, Pelletier JH, et al. (1983) Shear strength interpretation for Gulf of Mexico clays. *Geotech Pract Offshore Eng*, 144–165.
3. Mayne PW, Peuchen J (2018) Evaluation of CPTU N_{kt} cone factor for undrained strength of clays, *Cone Penetration Testing 2018*. The Netherlands: Delft University of Technology, 423–429.
4. Agaiby SS, Mayne PW (2019) CPT evaluation of yield stress profiles in soils. *J Geotech Geoenviron Eng* 145: 04019104. https://doi.org/10.1061/(ASCE)GT.1943-5606.0002164
5. Mayne PW, Peuchen J, Baltoukas D (2015) Piezocone evaluation of undrained strength in soft to firm offshore clays. *Front Offshore Geotechnics III* 1: 1091–1096.

6. Quiros GW, Little RL, Garmon S (2000) A normalized soil parameter procedure for evaluating in-situ shear strength. *Annu Offshore Technol Conf*. Houston, Texas, USA. https://doi.org/10.4043/12090-MS
7. Casey B, Germaine JT (2013) Stress dependence of shear strength in fine-grained soils and correlations with liquid limit. *J Geotech Geoenviron Eng.* 139: 1709–1717.
8. Yang SL, Lunne T, Santos R, et al. (2015) Strength parameters for suction anchors in a high plasticity Ghana clay. *3rd Int Symp Front Offshore Geotechnics* 139: 1139–1144.
9. Ladd CC, Foott R (1974) New design procedure for stability of soft clay. *J Geotech Eng* 100: 763–786.
10. Zhang G, Germaine JT, Whittle AJ (2003) Effects of fe-oxides cementation on the deformation characteristics of a highly weathered old alluvium in San Juan, Puerto Rico. *Soils Found* 43: 119–130. https://doi.org/10.3208/sandf.43.4_119
11. Burland JB (1990) On the compressibility and shear strength of natural soils. *Géotechnique* 40: 329–378.
12. Robertson PK, Cabal KL (2015) *Guide to cone penetration testing for geotechnical engineering*. Gregg Drilling & Testing, Inc., 6th Edition, Signal Hill, California, USA.
13. Rad NS, Lunne T (1986) Correlations between piezocone results and laboratory soil properties. *Norw Geotech Inst*, 306–317.
14. Lunne T, Anderson KH, Yang SL, et al. (2013) Undrained shear strength for foundation design at the Luva deep water field in the Norwegian Sea. *Geotech Geophys Site Charact* 1: 157–166.
15. Stevens RF, Millan C, Gupta U, et al. (2022) Pile Driving in Heavily Overconsolidated Clays. *Annu Offshore Technol Conf*. Houston, Texas, USA. https://doi.org/10.4043/31834-MS
16. L'Heureux JS, Lindgård A, Emdal E (2019) The Tiller-Flotten research site: Geotechnical characterization of a very sensitive clay deposit. *AIMS Geosci* 5: 831–867. https://doi.org/10.3934/geosci.2019.4.831
17. Gundersen AS, Hansen RC, Lunne T, et al. (2019) Characterization and engineering properties of the NGTS Onsøy soft clay site. *AIMS Geosci* 5: 665–703. https://doi.org/10.3934/geosci.2019.3.665
18. Helle TE, Aagaard P, Nordal S, et al. (2019) A geochemical, mineralogical, and geotechnical characterization of the low plastic, highly sensitive glaciomarine clay at Dragvoll, Norway. *AIMS Geosci* 5: 704–722. https://doi.org/10.3934/geosci.2019.4.704
19. Blaker Ø, Carroll RP, Paniagua P, et al. (2019) Halden research site: geotechnical characterization of a post glacial silt. *AIMS Geosci* 5: 184–234. https://doi.org/10.3934/geosci.2019.2.184
20. Bihs A, Long M, Nordal S (2020) Geotechnical characterization of Halsen-Stjørdal silt, Norway. *AIMS Geosci* 6: 355–377. https://doi.org/10.3934/geosci.2020020
21. Larsson R (2001) Investigations and load tests in clay till. Results from a series of investigations and load tests in the test field at Tornhill outside Lund in southern Sweden. Swedish Geotechnical Institute, Linköping, Sweden.
22. Di Buò B, D'Ignazio M, Selänpää J, et al. (2019) Investigation and geotechnical characterization of Perniö clay, Finland. *AIMS Geosci* 5: 591–616. https://doi.org/10.3934/geosci.2019.3.591
23. Nash DFT, Powell JJM, Lloyd IM (1992) Initial investigations of the soft clay test site at Bothkennar. *Géotechnique* 42: 163–181. https://doi.org/10.1680/geot.1992.42.2.163
24. Zdravcovic L, Jardine R, Taborda DMG, et al. (2020) Ground characterisation for PISA pile testing and analysis. *Géotechnique* 70: 945–960. https://doi.org/10.1680/jgeot.18.PISA.001

25. Radaszewski R, Wierzbicki J (2019) Characterization and engineering properties of AMU Morasko soft clay. *AIMS Geosci* 5: 235–264. https://doi.org/10.3934/geosci.2019.2.235
26. Mayne PW, Cargill E, Miller B (2019) Geotechnical characteristics of sensitive Leda clay at Canada test site in Gloucester, Ontario. *AIMS Geosci* 5: 390–411. https://doi.org/10.3934/geosci.2019.3.390
27. Kavur B, Mulabdic M, Minazek K (2010) Evaluation of piezocone characterization in deltaic deposits. *2nd Intern Symp on Cone Penetration Testing* 2: 281–288.
28. Mayne P, Benoit J (2020) Analytical CPTU models applied to sensitive clay at Dover, New Hampshire. *J Geotech Geoenviron Eng* 146: 04020130. https://doi.org/10.1061/(ASCE)GT.1943-5606.0002378
29. DeGroot DJ, Landon ME, Poirier SE (2019) Geology and engineering properties of sensitive Boston Blue Clay at Newbury, Massachusetts. *AIMS Geosci* 5: 412–447. https://doi.org/10.3934/geosci.2019.3.412
30. Liedtke E, Jeanjean P, Humphrey GD (2006) Geotechnical site investigation for the Mad Dog spur anchors. *38th Annu Offshore Technol Conf.* Houston, Texas, USA.
31. Schroder K, Andersen KH, Tjok KM (2006) Laboratory testing and detailed geotechnical design of the mad dog anchors. *38th Annu Offshore Technol Conf.* Houston, Texas, USA. https://doi.org/10.4043/17949-MS
32. Giao P, Nguyen T, Long P (2008) An integrated geotechnical-geophysical investigation of soft clay at a coastal site in the Mekong Delta for oil and gas infrastructure development. *Can Geotech J* 45: 1514–1524. https://doi.org/10.1139/T08-077
33. Ozkul ZH, Remmes B, Bik M (2013) Piezocone profiling of a deepwater clay site in the Gulf of Guinea. *45th Annu Offshore Technol Conf*. Houston, Texas, USA. https://doi.org/10.4043/24136-MS
34. Trevor FA, Paisley JM, Konda Y, et al. (2008) Soil properties of deepwater sediments in the Timor Sea. *Proc Geotech Geophys Site Charact*. London: Taylor & Francis Group. 551–558.
35. Danziger FAB, Jannuzzi GMF, Toniazzo MVCMV, et al. (2015) DMT tests at Sarapui soft clay deposit: from 1985 to 2012. *3rd Intern Conf Flat Dilatometer DMT*, 465–472.
36. Pineda JA, Kelly RB, Suwal L, et al. (2019) The Ballina soft soil field testing facility. *AIMS Geosci* 5: 509–534. https://doi.org/10.3934/geosci.2019.3.509
37. Low HE, Lunne T, Andersen KH, et al. (2010) Estimation of intact and remoulded undrained shear strengths from penetration tests in soft clays. *Géotechnique* 60: 843–859. https://doi.org/10.1680/geot.9.P.017
38. Casagrande A (1936) Determination of preconsolidation load and its practical significance. *First Int Conf Soil Mech Found Eng* 3: 60–64.

Appendix

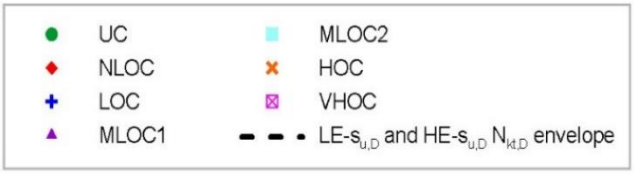

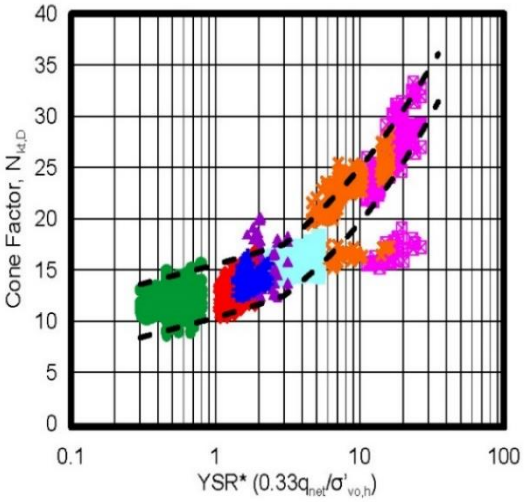

Figure A1. $N_{kt,D}$ versus YSR* by location using all methods

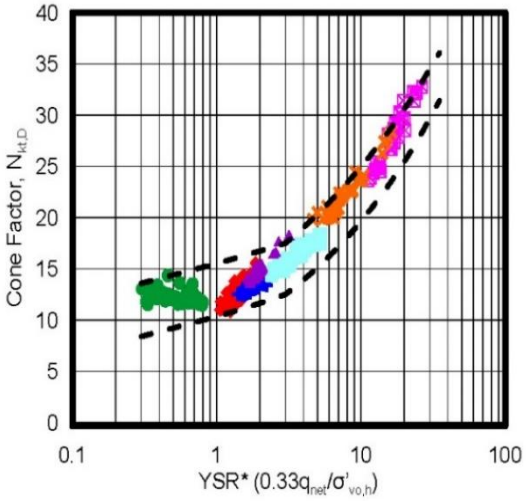

Figure A2. $N_{kt,D}$ ($8.2Q_u^{0.3}$) versus YSR*

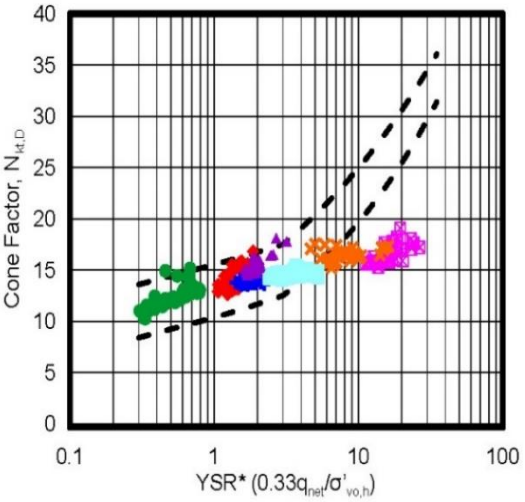

Figure A3. $N_{kt,D}$ [10.5-4.6*ln(B_q+0.1)] versus YSR*

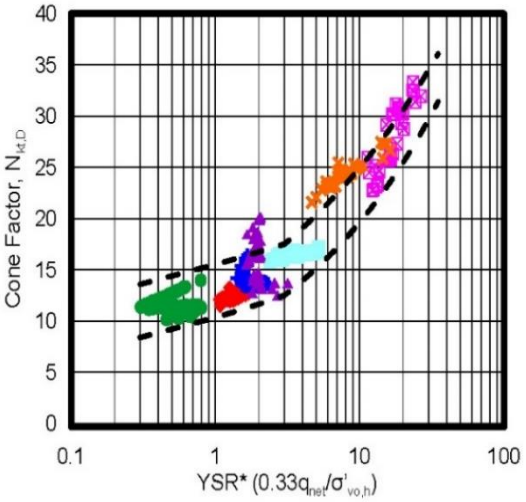

Figure A4. $N_{kt,D}$ $[\sigma'_{vo}S_1(\sigma'_p)^T(OCR^m]$ versus YSR*

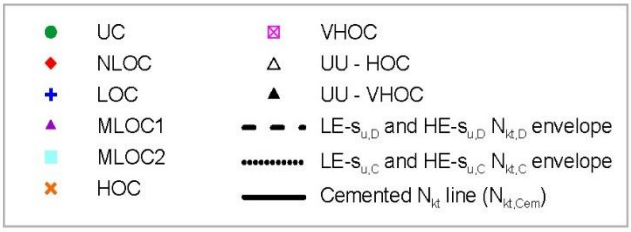

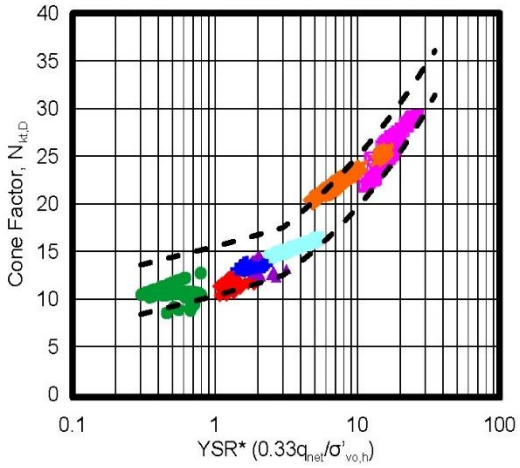

Figure A5. $N_{kt,D}$ (derived from $s_{u,SP}$) versus YSR*

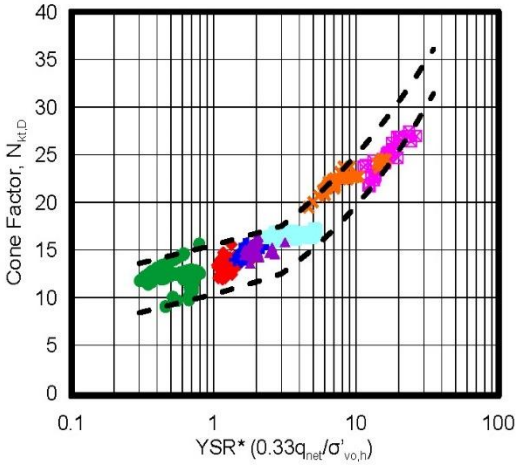

Figure A6. $N_{kt,D}$ (derived from $s_{u,SPLI}$) versus YSR*

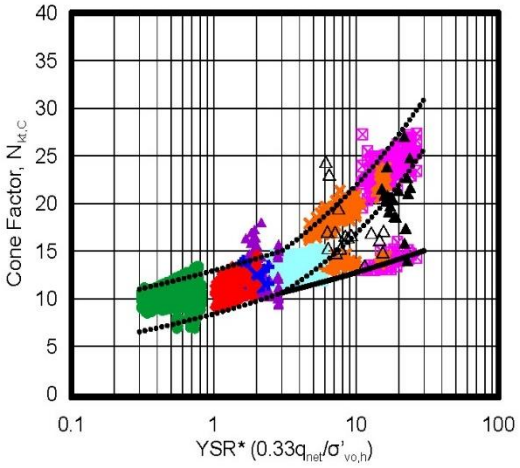

Figure A7. $N_{kt,C}$ and $N_{kt,Cem}$ versus YSR*

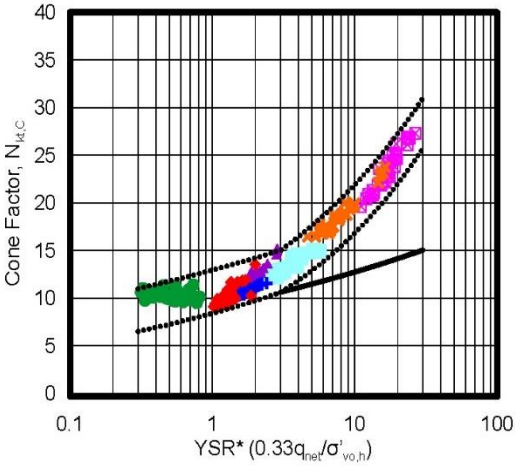

Figure A8. $N_{kt,C}$ ($8.2Q_u^{0.3}$) versus YSR*

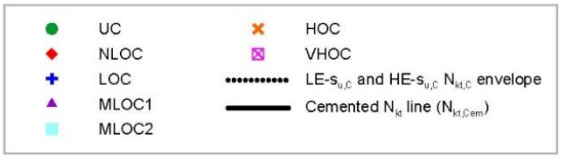

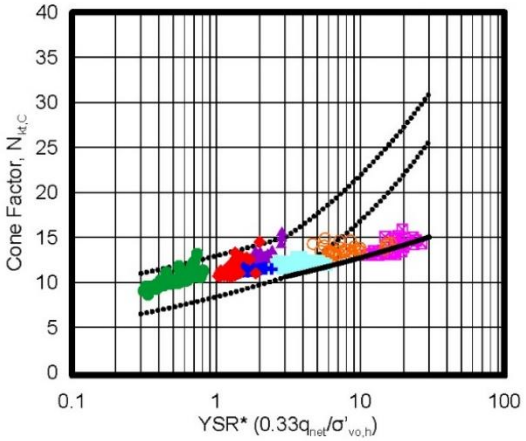

Figure A9. $N_{kt,c}$ [10.5-4.6*ln(B_q+0.1)] versus YSR*

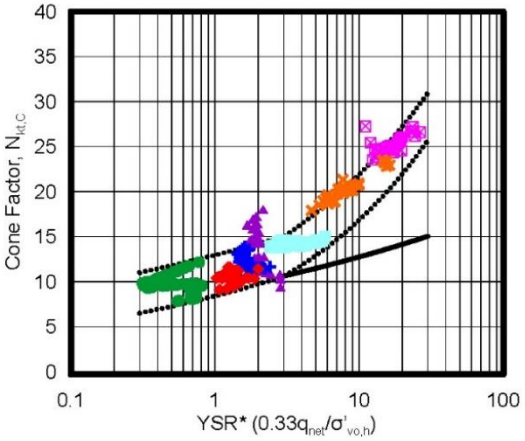

Figure A10. $N_{kt,c}$ [$\sigma'_{vo}S^1(\sigma'_p)^T(OCR^m)$] versus YSR*

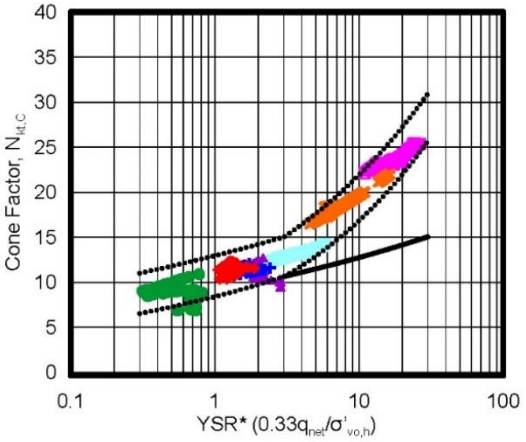

Figure A11. $N_{kt,C}$ (derived from $s_{u,SP}$) versus YSR*

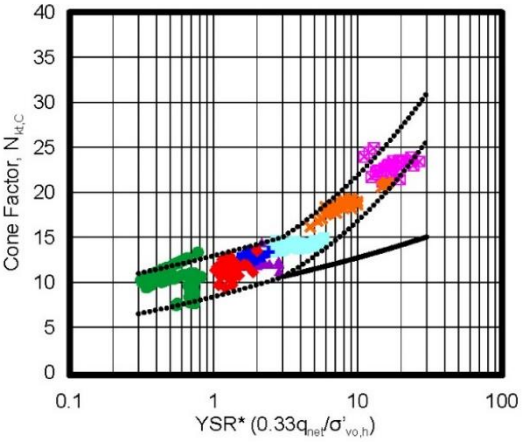

Figure A12. $N_{kt,C}$ (derived from $s_{u,SPLI}$) versus YSR*

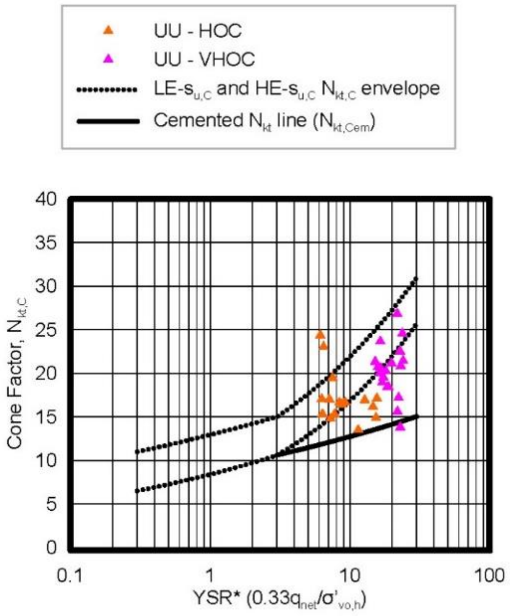

Figure A13. $N_{kt,c}$ (derived from $s_{u,UU}$) versus YSR*

Table A1: Modified equations for the $N_{kt,D}$–$q_{net}/\sigma'_{vo,h}$ and $N_{kt,C}$–$q_{net}/\sigma'_{vo,h}$ correlations without the "0.33" term.

Application range	$s_{u,D}$-based equation	$s_{u,C}$-based equation
$q_{net}/\sigma'_{vo,h} \leq 9.1$	LE-$s_{u,D}$ $N_{kt,D} = 13.73(q_{net}/\sigma'_{vo,h})^{0.11}$	LE-$s_{u,C}$ $N_{kt,C} = 11.14(q_{net}/\sigma'_{vo,h})^{0.135}$
$q_{net}/\sigma'_{vo,h} > 9.1$	LE-$s_{u,D}$ $N_{kt,D} = 9.15(q_{net}/\sigma'_{vo,h})^{0.294}$	LE-$s_{u,C}$ $N_{kt,C} = 7.48(q_{net}/\sigma'_{vo,h})^{0.315}$
$q_{net}/\sigma'_{vo,h} \leq 9.1$	HE-$s_{u,D}$ $N_{kt,D} = 8.54(q_{net}/\sigma'_{vo,h})^{0.173}$	HE-$s_{u,C}$ $N_{kt,C} = 6.64(q_{net}/\sigma'_{vo,h})^{0.212}$
$q_{net}/\sigma'_{vo,h} > 9.1$	HE-$s_{u,D}$ $N_{kt,D} = 5.46(q_{net}/\sigma'_{vo,h})^{0.375}$	HE-$s_{u,C}$ $N_{kt,C} = 4.53(q_{net}/\sigma'_{vo,h})^{0.385}$
*$q_{net}/\sigma'_{vo,h} > 9.1$	—	$N_{kt,Cem} = 7.61(q_{net}/\sigma'_{vo,h})^{0.151}$

*Cemented cohesive soil